Letter

A Novel Scalable Fault-Tolerant Control Design for DC Microgrids With Nonuniform Faults

Aimin Wang, Minrui Fei, Dajun Du, and Yang Song

Dear Editor,

The existing control schemes for microgrids (MGs) face challenges in effectively addressing plugging in/out operations under uncertain power lines and faults. To tackle this issue, this letter proposes a novel scalable fault-tolerant control (FTC) strategy for DC MGs. By developing a structured Lyapunov matrix (SLM), a decoupled FTC method is introduced to mitigate the adverse effects of uncertain lines and nonuniform faults. Moreover, global stability is ensured by deriving local rules expressed as linear matrix inequalities (LMIs) that solely depend on local parameters. Each new distributed generation unit (DGU) introduces only one additional condition of this nature, allowing the stability rules to scale with topology changes. Finally, the effectiveness of the proposed scheme is illustrated through simulations conducted using the MATLAB/SimPowerSystems toolbox.

In contrast to AC MGs [1], DC MGs do not face issues related to reactive power and frequency control. Additionally, due to their ease of management, higher efficiency, sustainability, and lower carbon dioxide emissions, DC MGs have found applications in various domains, such as electric vehicles and marine systems [2]. However, the demand for plug-and-play (PnP) operations and the application of power devices present two fundamental challenges for MGs, namely, topology changes [2] and component faults [3].

On one hand, the topology structure of a system (e.g., automated vehicles and MGs) often changes due to PnP requirements [4], [5]. Specifically, in MGs, the computational demand increases as topology changes, resulting in transient processes. Decentralized PnP (DPnP) has emerged as a prevailing scalable control method employed in MGs. For instance, Tucci *et al.* [6] proposed a DPnP control approach based on information about local DGUs and power lines. Although existing DPnP methods (e.g., [6]) enable PnP operations, their scalability may be limited as line parameters are often uncertain [7]. Consequently, there is a motivation to propose a new scalable control scheme to address the challenges posed by uncertain lines.

Another key aspect related to MGs is component faults. The voltage source converter (VSC) comprises various power electronic components, such as IGBT, SCR, or MOSFET, which are highly susceptible to faults, including packaging failures, open-circuit, and short-circuits. These faults can cause a loss of control effectiveness (LoCE) [3]. FTC methods have been widely used in MGs to tolerate LoCE faults [8], [9]. However, existing FTC schemes, assuming uniformly distributed faults in [8], [9], may exhibit conservatism since LoCE faults in VSCs are practically nonuniform [3]. Note that [3] shows that LoCE faults can be divided into catastrophic and wear-out types with different distribution probabilities. To the best of the authors' knowledge, there is limited research characterizing the effects of such nonuniform LoCE faults, particularly in the context of achieving scalable performance. This knowledge gap serves as another motivation for the present study.

This letter proposes a novel scalable FTC scheme for DC MGs with nonuniform faults, enabling DGUs to be plugged in/out over time. The main contributions are summarized as follows: 1) A novel SLM-based FTC method is proposed to eliminate the adverse effects of uncertain lines and nonuniform faults. 2) The stability of global MGs is ensured by deriving the local rules that involve only their own local parameters, thereby enabling the proposed scalable FTC scheme to adapt to topology changes.

Corresponding authors: Aimin Wang and Minrui Fei.

Citation: A. Wang, M. Fei, D. Du, and Y. Song, "A novel scalable fault-tolerant control design for DC microgrids with nonuniform faults," *IEEE/CAA J. Autom. Sinica*, vol. 11, no. 8, pp. 1886–1888, Aug. 2024.

The authors are with the Shanghai Key Laboratory of Power Station Automation Technology, the School of Mechatronic Engineering and Automation, Shanghai University, Shanghai 200072, China (e-mail: amwang@shu.edu.cn; mrfei@staff.shu.edu.cn; ddi@i.shu.edu.cn; y_song@shu.edu.cn).

Color versions of one or more of the figures in this paper are available online at http://ieeexplore.ieee.org.

Digital Object Identifier 10.1109/JAS.2023.123918

Problem statement: As depicted in Fig. 1, we consider a simplified DC MGs comprising n agents. The agents $i \in \mathbb{N} \triangleq \{1,\ldots,n\}$ are interconnected with their neighbors $j \in \mathcal{N}_i \subset \mathbb{N}$ via power line Z_{ij}. Each power line is characterized by a nonzero impedance (R_{ij}, L_{ij}). Each agent includes a DC voltage source (representing a generic renewable source), a VSC controlled by a local controller, and a resistive load R_{Li} connected to PCC$_i$ through a series RLC filter with parameters R_{ti}, L_{ti} C_{ti} [6].

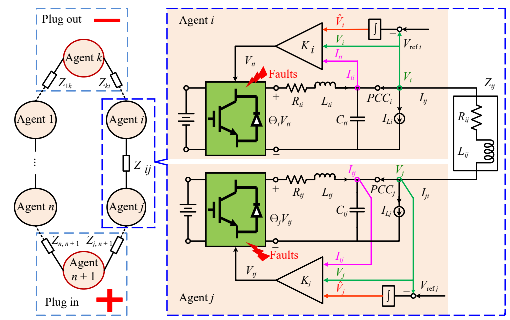

Fig. 1. Framework of scalable FTC control for DC MGs with faults.

Applying Kirchhoff voltage and current laws to Fig. 1 and QSL technique [7], the ith electrical model can be obtained as

$$\begin{cases} \dot{V}_i = \dfrac{1}{C_{ti}} I_{ti} + \sum_{j\in\mathcal{N}_i} \dfrac{1}{C_{ti}R_{ij}} \left(V_j - V_i\right) - \dfrac{1}{C_{ti}R_{Li}} V_i \\ \dot{I}_{ti} = -\dfrac{R_{ti}}{L_{ti}} I_{ti} - \dfrac{1}{L_{ti}} V_i + \dfrac{1}{L_{ti}} V_{ti} \end{cases} \tag{1}$$

where V_i and V_j denote voltage signals at PCC$_i$ and PCC$_j$, respectively. I_{ti} is filter current and V_{ti} denotes control signal to VSC.

To eliminate the steady-state error in voltage tracking, an integrator is incorporated into each agent of the MGs, following the format:

$$\dot{\widehat{V}}_i = V_{\text{ref}i} - V_i \tag{2}$$

where $\widehat{V}_i$ and $V_{\text{ref}i}$ are the integrated voltage error and reference voltage. Combining (1) and (2), the ith local subsystem can be denoted as the following state-space model:

$$\begin{cases} \dot{x}_i(t) = A_{ii}x_i(t) + B_i u_i^F(t) + W_i w_i(t) + \xi_i(t) \\ y_i(t) = C_i x_i(t) \end{cases} \tag{3}$$

where $x_i(t) = \text{col}\{V_i, I_{ti}, \widehat{V}_i\}$, $y_i(t) = V_i$, and $u_i^F(t)$ denote the state, output, and actual input vector of DGUi, respectively. $w_i(t) = V_{\text{ref}i}$ is seemed as the bounded disturbance [10]. $\xi_i(t) = \sum_{j\in\mathcal{N}_i} A_{ij}(x_j - x_i)$ denotes line coupling between DGUs. Besides,

$$A_{ii} = \begin{bmatrix} -\dfrac{1}{C_{ti}R_{Li}} & \dfrac{1}{C_{ti}} & 0 \\ -\dfrac{1}{L_{ti}} & -\dfrac{R_{ti}}{L_{ti}} & 0 \\ -1 & 0 & 0 \end{bmatrix}, \ A_{ij} = \begin{bmatrix} \dfrac{1}{R_{ij}C_{ti}} & 0 & 0 \\ 0 & 0 & 0 \\ 0 & 0 & 0 \end{bmatrix}$$

$$B_i = \left[0,\ \frac{1}{L_{ti}},\ 0\right]^T,\ C_i = [1,\ 0,\ 0],\ W_i = [0,\ 0,\ 1]^T.$$

Scalable fault-tolerant controller design: The local controller of interest is defined as follows:

$$V_{ti} = K_i x_i \tag{4}$$

where $K_i = [K_{1i}\ K_{2i}\ K_{3i}]$ represents the controller gains, which will be designed in the sequel.

In contrast to the existing uniform LoCE faults [8], [9], characterized by $u_i^F(t) = \theta_i u_i(t)$, $0 \le \theta_i \le 1$, we model the considered nonuniform faults with different distribution probabilities as follows:

$$u_i^F(t) = \Theta_i V_{ti}(t), \quad \Theta_i = \eta_i(t)\widehat{\theta}_i + (1-\eta_i(t))\widetilde{\theta}_i \tag{5}$$

where $\widehat{\theta}_i \in [0, \bar{\theta}_i)$ represents the fault efficiency of catastrophic LoCE fault (CLF), and $\widetilde{\theta}_i \in [\bar{\theta}_i, 1]$ denotes the fault efficiency of wear-out LoCE fault (WLF). Here, $\bar{\theta}_i \in (0,1)$ is a given scalar that properly divides the set of fault efficiencies $[0,1]$ into two subsets: $[0,\overline{\theta}_i)$ and $[\overline{\theta}_i,1]$. Furthermore, $\eta_i(t)$ is a Bernoulli-distributed variable that characterizes the likelihood of a fault belonging to either WLF or CLF in different VSCs. Hence, the following statistical properties can be given:

$$\begin{aligned} \text{Prob}\{\eta_i(t)=1\} &= \mathcal{E}\{\eta_i(t)\} = \overline{\eta}_i \\ \text{Prob}\{\eta_i(t)=0\} &= 1-\mathcal{E}\{\eta_i(t)\} = 1-\overline{\eta}_i. \end{aligned} \tag{6}$$

Remark 1: Note that nonuniform LoCE faults in VSCs can be characterized by the Bernoulli variable $\eta_i(t) \in [0,1]$, which indicates the probability of a LoCE fault being classified as CLF or WLF at a given time instant t. Specifically, when $\eta_i(t)=1$, i.e., $\Theta_i = \widehat{\theta}_i$, it implies the occurrence of CLF, whereas $\eta_i(t)=0$, i.e., $\Theta_i = \widetilde{\theta}_i$, denotes the existence of WLF. In practical scenarios, WLF tends to manifest more frequently than CLF, and the detrimental impact of CLF on the system is more pronounced than that of WLF.

Therefore, the closed-loop global MGs, composed of n agents, can be described as follows:

$$\mathbb{S}_{gl}: \begin{cases} \dot{\boldsymbol{x}}(t) = (\boldsymbol{A}+\boldsymbol{B\Theta K})\boldsymbol{x}(t) + \boldsymbol{W}\boldsymbol{w}(t) \\ \boldsymbol{y}(t) = \boldsymbol{C}\boldsymbol{x}(t) \end{cases} \tag{7}$$

where $A = \left[A_{ij}\right]_{i,j\in\mathbb{N}}$, and

$$\begin{aligned} &\boldsymbol{x}(t) = \text{col}\{x_1(t),\ldots,x_n(t)\}, \quad \boldsymbol{y}(t) = \text{col}\{y_1(t),\ldots,y_n(t)\} \\ &\boldsymbol{w}(t) = \text{col}\{w_1(t),\ldots,w_n(t)\}, \quad \boldsymbol{B} = \text{diag}\{B_1,\ldots,B_n\} \\ &\boldsymbol{C} = \text{diag}\{C_1,\ldots,C_n\}, \quad \boldsymbol{W} = \text{diag}\{W_1,\ldots,W_n\} \\ &\boldsymbol{\Theta} = \text{diag}\{\Theta_1,\ldots,\Theta_n\}, \quad \boldsymbol{K} = \text{diag}\{K_1,\ldots,K_n\}. \end{aligned}$$

By observing the structure of $\boldsymbol{A}$, it can be decomposed as

$$\boldsymbol{A} = \boldsymbol{A}_v - (\boldsymbol{A}_d - \boldsymbol{A}_a) \tag{8}$$

where $\boldsymbol{A}_v = \text{diag}\{A_{11},\ldots,A_{ii},\ldots,A_{nn}\}$ represents the collection of local dynamics information, and A_d denotes the dependence of each local state on the neighboring agents, given by $\boldsymbol{A}_d = \text{diag}\{A_{d1},\ldots,A_{di},\ldots,A_{dn}\}$ with the following format:

$$A_{di} = \left[\begin{array}{c|c} \sum_{j\in\mathcal{N}_i} \dfrac{1}{R_{ij}C_{ti}} & \mathbf{0}^{1\times 2} \\ \hline * & \mathbf{0}^{2\times 2} \end{array}\right]. \tag{9}$$

Additionally, $\boldsymbol{A}_a$ denotes the effect of line coupling, comprising zero blocks on the diagonal and blocks A_{ij}, $\forall j \neq i$ outside the diagonal.

Subsequently, the following definition is introduced, which is essential for deriving the main results presented in this letter.

Definition 1 [3]: A closed-loop system with $w_i(t) \in \mathcal{L}_2[0,\infty)$ is said to have an H_∞ performance level γ_i, if it satisfies the following condition under zero initial state:

$$\int_0^\infty y_i^T(t)y_i(t)dt < \gamma_i^2 \int_0^\infty w_i^T(t)w_i(t)dt.$$

Main results: This section aims to design a scalable FTC scheme for MGs. Firstly, Lemma 1 presents a stability criterion for the local subsystem without line coupling $\sum_{j\in\mathcal{N}_i} A_{ij}(x_j - x_i)$. However, this stability criterion cannot be assured in the presence of line coupling. Thus, Theorem 1 proposes an SLM-based Laplacian decoupled method to eliminate the negative effect of line coupling. Finally, Theorem 2 presents a design approach for a scalable FTC scheme.

The following is the statement of Lemma 1.

Lemma 1: The ith local subsystem is asymptotically stable with an H_∞ performance level γ_i, if there exists a Lyapunov function $V_i(x_i(t)) = x_i^T(t)P_i x_i(t)$ with $P_i = P_i^T > 0$, such that the following condition holds:

$$\begin{bmatrix} A_{ii}^T P_i + P_i A_{ii} + \Xi_i & P_i W_i & C_i^T \\ * & -\gamma_i^2 I & 0 \\ * & * & -I \end{bmatrix} < 0 \tag{10}$$

where $\Xi_i = K_i^T \overline{\Theta}_i B_i^T P_i + P_i B_i \overline{\Theta}_i K_i$, $\overline{\Theta}_i = \overline{\eta}_i \widehat{\theta}_i + (1-\overline{\eta}_i)\widetilde{\theta}_i$.

Proof: The proof steps are well known and involve Definition 1. Due to space limitations, the complete proof is omitted. ■

Next, we will introduce the following assumption that plays a crucial role in the SLM-based Laplacian decoupled method.

Assumption 1: The local controller K_i (4) is designed based on a SLM P_i with the following structure:

$$P_i = \left[\begin{array}{c|c} \rho_i & \mathbf{0}^{1\times 2} \\ \hline \mathbf{0}^{2\times 1} & \mathcal{P}_i \end{array}\right] \tag{11}$$

where $\mathcal{P}_i \in \mathbb{R}^{2\times 2}$ denotes an arbitrary matrix, and $\rho_i = \lambda_i C_{ti}$ with a given positive scalar λ_i.

The global stability criterion will be presented using the SLM-based Laplacian decoupled method to eliminate line coupling.

Theorem 1: The global MGs $\mathbb{S}_{gl}$ is asymptotically stable with H_∞ performance level $\boldsymbol{\gamma} = \text{diag}\{\gamma_1,\ldots,\gamma_n\}$, if there exists a positive definite matrix $\boldsymbol{P} = \text{diag}\{P_1,\ldots,P_n\}$ with entry P_i defined in (11), such that the following condition holds:

$$\begin{bmatrix} \boldsymbol{A}^T\boldsymbol{P} + \boldsymbol{PA} + \boldsymbol{\Xi} & \boldsymbol{PW} & \boldsymbol{C}^T \\ * & -\boldsymbol{\gamma}^2 I & \mathbf{0}^{n\times n} \\ * & * & -I \end{bmatrix} < 0 \tag{12}$$

where

$$\begin{aligned} &\boldsymbol{\Xi} = \boldsymbol{K}^T\boldsymbol{\Theta}^T\boldsymbol{B}^T\boldsymbol{P}^T + \boldsymbol{PB\Theta K}, \quad \boldsymbol{\Theta} = \overline{\eta}\widehat{\boldsymbol{\theta}} + (I-\overline{\eta})\widetilde{\boldsymbol{\theta}} \\ &\overline{\eta} = \text{diag}\{\overline{\eta}_1,\ldots,\overline{\eta}_n\}, \quad \widehat{\boldsymbol{\theta}} = \text{diag}\{\widehat{\theta}_1,\ldots,\widehat{\theta}_n\}, \quad \widetilde{\boldsymbol{\theta}} = \text{diag}\{\widetilde{\theta}_1,\ldots,\widetilde{\theta}_n\}. \end{aligned}$$

Proof: According to (8), $\boldsymbol{A}^T\boldsymbol{P} + \boldsymbol{PA}$ can be rewritten as

$$\boldsymbol{A}^T\boldsymbol{P} + \boldsymbol{PA} = \boldsymbol{A}_v^T\boldsymbol{P} + \boldsymbol{PA}_v - \left(\overbrace{\underbrace{\boldsymbol{A}_d^T\boldsymbol{P} + \boldsymbol{PA}_d}_{term(1)} - (\underbrace{\boldsymbol{A}_a^T\boldsymbol{P} + \boldsymbol{PA}_a}_{term(2)})}^{term(3)}\right). \tag{13}$$

Firstly, collecting the Lyapunov function $V_i(x_i(t))$, one has $\boldsymbol{V}(\boldsymbol{x}(t)) = \sum_{i=1}^n V_i(x_i(t)) = \boldsymbol{x}^T(t)\boldsymbol{P}\boldsymbol{x}(t)$. Recalling (10) in Lemma 1, one obtains

$$\begin{bmatrix} \boldsymbol{A}_v^T\boldsymbol{P} + \boldsymbol{PA}_v + \boldsymbol{\Xi} & \boldsymbol{PW} & \boldsymbol{C}^T \\ * & -\boldsymbol{\gamma}^2 I & \mathbf{0}^{n\times n} \\ * & * & -I \end{bmatrix} < 0. \tag{14}$$

Then, remanding (9) and (11), it can be shown that the $term(1)$ in (13) is block diagonal, with each block represented by $A_{di}^T P_i + P_i A_{di}$ in the following form:

$$A_{di}^T P_i + P_i A_{di} = \left[\begin{array}{c|c} \sum_{j\in\mathcal{N}_i} \dfrac{2\lambda_i}{R_{ij}} & \mathbf{0}^{1\times 2} \\ \hline \mathbf{0}^{2\times 1} & \mathbf{0}^{2\times 2} \end{array}\right]. \tag{15}$$

It is evident that only the element at position (1, 1) of (15) is nonzero, while all other entries are zero. Let L_{ii} denote the item obtained by deleting the last two rows and columns of (15), yielding $L_{ii} = \sum_{j\in\mathcal{N}_i} \frac{2\lambda_i}{R_{ij}}$. By defining a diagonal matrix $\mathcal{D}$ to collect the aforementioned modified blocks of the $term(1)$, one obtains $\mathcal{D} = \text{diag}\{L_{11},\ldots,L_{ii},\ldots,L_{nn}\}$. Furthermore, when $i\in\mathbb{N}, j\in\mathcal{N}_i$, each block in position (i,j) of the $term(2)$ in (13) can be described as $A_{ji}^T P_j + P_i A_{ij}$. By combining the matrices A_{ij} and P_i in (11), one has

$$A_{ji}^T P_j + P_i A_{ij} = \left[\begin{array}{c|c} \dfrac{2\lambda_i}{R_{ij}} & \mathbf{0}^{1\times 2} \\ \hline \mathbf{0}^{2\times 1} & \mathbf{0}^{2\times 2} \end{array}\right]. \tag{16}$$

Similarly, by defining L_{ij} to denote an item obtained by deleting the zero entries of (16) (i.e., the last two rows and columns), one has $L_{ij} = \frac{2\lambda_i}{R_{ij}}$ if $i\in\mathbb{N}, j\in\mathcal{N}_i$; otherwise, $L_{ij} = 0$. By defining a symmetric matrix $\mathcal{A}$ to collect the modified blocks of the $term(2)$ and defining $\mathcal{L} = \mathcal{D} - \mathcal{A}$, one can obtain matrices $\mathcal{A}$ and $\mathcal{L}$ with the following structure:

$$\mathcal{A} = \begin{bmatrix} 0 & L_{12} & \cdots & L_{1n} \\ L_{21} & 0 & \cdots & L_{2n} \\ \vdots & \vdots & \ddots & \vdots \\ L_{n1} & L_{n2} & \cdots & 0 \end{bmatrix}, \quad \mathcal{L} = \begin{bmatrix} L_{11} & -L_{12} & \cdots & -L_{1n} \\ -L_{21} & L_{22} & \cdots & -L_{2n} \\ \vdots & \vdots & \ddots & \vdots \\ -L_{n1} & -L_{n2} & \cdots & L_{nn} \end{bmatrix}.$$

Thus, it can be concluded that the attribute about positiveness/negativeness of the $term(3)$ in (13) can be investigated through $\mathcal{L}$, which can be regarded as the structure of a Laplacian matrix. In this regard, $\mathcal{L}$ is positive semi-definite, that is $-\mathcal{L} \leq 0$. Therefore, the following inequality holds:

$$\left[\begin{array}{c|c} \boldsymbol{A}_d^T\boldsymbol{P} - \boldsymbol{A}_a^T\boldsymbol{P} + \boldsymbol{PA}_d - \boldsymbol{PA}_a & \mathbf{0}^{3n\times 2n} \\ \hline \mathbf{0}^{2n\times 3n} & \mathbf{0}^{2n\times 2n} \end{array}\right] \leq 0 \tag{17}$$

Accoding to $\boldsymbol{A} = \boldsymbol{A}_v - (\boldsymbol{A}_d - \boldsymbol{A}_a)$ in (8), (12) can be derived by combinating (14) and (17). ■

Remark 2: Theorem 1 presents a sufficient condition for ensuring the asymptotic stability of global MGs (7) in the presence of line coupling. Note that the proposed SLM-based Laplacian decoupled method eliminates line coupling among DGUs. As a result, the stability criterion exclusively relies on the local information of the DGUs themselves, without considering the electrical parameters of power line, particularly when they are not uncertain.

Next, a design approach for a scalable FTC scheme is presented.

Theorem 2: The ith local subsystem is asymptotically stable with an H_∞ performance level γ_i, if there exist matrices Y_i and G_i, such that the following conditions hold:

$$\begin{bmatrix} \Phi_i & W_i & Y_i C_i^T \\ * & -\overline{\gamma}_i I & 0 \\ * & * & -I \end{bmatrix} < 0 \quad (18a)$$

$$\begin{bmatrix} -\beta_i I & G_i^T \\ * & -I \end{bmatrix} < 0, \quad \begin{bmatrix} Y_i & I \\ * & \alpha_i I \end{bmatrix} > 0 \quad (18b)$$

$$Y_i = \left[\begin{array}{c|c} \frac{1}{\rho_i} & \mathbf{0}^{1\times 2} \\ \hline \mathbf{0}^{2\times 1} & \mathcal{Y}_i \end{array}\right] > 0 \quad (18c)$$

where $\Phi_i = Y_i A_{ii}^T + A_{ii} Y_i + G_i^T \overline{\Theta}_i^T B_i^T + B_i \overline{\Theta}_i G_i$, $\overline{\gamma}_i = \gamma_i^2$, and $\mathcal{Y}_i \in \mathbb{R}^{2\times 2}$ is an arbitrary entry.

Thus, the scalable fault-tolerant controller K_i can be parameterized as $K_i = X_i Y_i^{-1}$ and be constrained by $\|K_i\|_2 < \sqrt{\beta_i}\alpha_i$.

Proof: By performing pre-multiplication and post-multiplication of (10) with $\text{diag}\{Y_i, I, I\}$, one can directly derive (18a). Furthermore, to prevent $\|K_i\|_2$ from becoming excessively large, which could compromise the performance of MGs, we consider the constraints $\|G_i\|_2 < \sqrt{\beta_i}$ and $\|Y_i^{-1}\|_2 < \alpha_i$. By applying the Schur complement to the constrained conditions, (18b) can be derived accordingly. ■

Remark 3: Note that the LMI-style conditions (22) consider the factor of fault efficiency $\overline{\Theta}_i = \overline{\eta}_i \widehat{\theta}_i + (1-\overline{\eta}_i)\widetilde{\theta}_i$, indicating the tolerance of the proposed controllers towards nonuniform faults. Moreover, these conditions solely depend on local information and remain unaffected by power parameters of lines, thereby demonstrating the scalability of the proposed controller design.

Numerical example: In this part, the effectiveness of the proposed control scheme is verified via numerical simulations using the MATLAB/SimPowerSystems toolbox. The considered MGs topology is depicted in Fig. 2, and the electrical parameters are adopted from [6]. For $\forall i = 1,2,3,4$, we set $\lambda_i = 10$, $\gamma_i = 0.1$, $\overline{\eta}_i = 0.2$, and $V_{\text{ref}i} = 50$ V, respectively. Additionally, fault efficiencies are respectively set to be $\widetilde{\theta}_1 = 0.9$, $\widetilde{\theta}_2 = 0.84$, $\widetilde{\theta}_3 = 0.8$, $\widetilde{\theta}_4 = 0.7$, $\widehat{\theta}_1 = 0.45$, $\widehat{\theta}_2 = 0.42$, $\widehat{\theta}_3 = 0.4$, $\widehat{\theta}_4 = 0.35$.

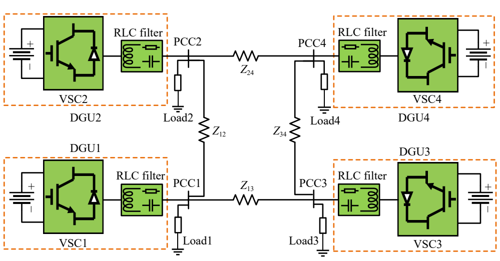

Fig. 2. The considered topology structure of MGs with four DGUs.

Based on these parameters, the controller gains K_i in Theorem 2 can be solved by using the MATLAB toolbox YALMIP, i.e.,

$$K_1 = [0.028\ \ -0.029\ \ 41.501],\ K_2 = [-0.001\ \ -0.018\ \ 98.682]$$
$$K_3 = [0.001\ \ -0.003\ \ 56.573],\ K_4 = [-0.001\ \ -0.018\ \ 99.874].$$

The simulation results are illustrated in Fig. 3, which includes Fig. 3(a) plug-in DGU 4 at $t = 2$ s, Fig. 3(b) plug-out DGU 4 at $t = 3$ s, Fig. 3(c) faults occur at $t = 4$ s, and Fig. 3(d) fault-tolerance performance against nonuniform faults by using method in [9]. From Figs. 3(a) and 3(b), it can be observed when DGU 4 is plugged in or out, voltage signals at PCCs deviate slightly from their references but quickly recover. Furthermore, Fig. 3(c) shows that voltage signals exhibit minor oscillations during nonuniform faults. Fig. 3(d) provides a comparative result using a common FTC method from [9], where the faults are assumed to have a uniform distribution. Clearly, voltage signals exhibit significant oscillations compared to their voltage references and fail to recover. These simulation results and comparisons demonstrate the effectiveness of the proposed scalable FTC scheme.

Conclusion: This letter has proposed a novel scalable FTC scheme for DC MGs to enable PnP operations under nonuniform faults. The adverse effects of uncertain power lines and nonuniform faults has been eliminated by developing a novel SLM-based FTC method. Furthermore, sufficient conditions have been presented to ensure the asymptotical stability of both local and global MGs, which were scalable with topology changes and tolerant to nonuniform faults. Finally, a numerical example conducted in MATLAB/SimPowerSystems toolbox has verified the proposed control scheme. In future research, it would be of considerable interest to extend the proposed scheme with a distributed architecture, incorporating communication networks to further enhance the reliability, robustness, and scalability of the system [11].

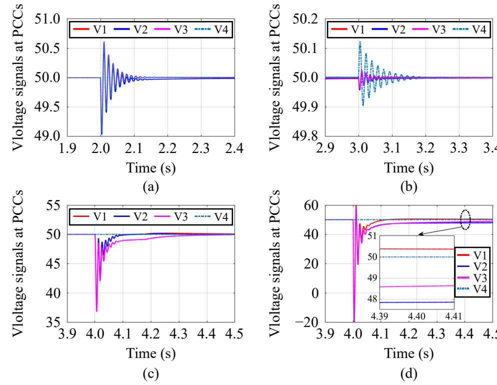

Fig. 3. Performance of the proposed scalable FTC scheme. (a) Plug-in DGU4 at $t = 2$ s; (b) Plug-out DGU4 at $t = 3$ s; (c) Faults occur at $t = 4$ s; (d) Fault-tolerance performance against nonuniform faults by using method in [9].

Acknowledgments: This work was supported by the Key Project of Science and Technology Commission of Shanghai Municipality (21190780300), the Natural Science Foundation of China (NSFC) (62173217, 62203290), the Natural Science Foundation of Shanghai Municipality (21ZR1423400), NSFC/Royal Society Cooperation and Exchange Project (62111530154), Shanghai Pujiang Program (22PJ 1403800), and 111 Project (D18003).

References

[1] B. Ning, Q.-L. Han, and L. Ding, "Distributed secondary control of AC microgrids with external disturbances and directed communication topologies: A full-order sliding-mode approach," *IEEE/CAA J. Autom. Sinica*, vol. 8, no. 3, pp. 554–564, Mar. 2021.

[2] C. Deng, F. Guo, C. Wen, D. Yue, and Y. Wang, "Distributed resilient secondary control for DC microgrids against heterogeneous communication delays and DoS attacks," *IEEE Trans. Ind. Electron.*, vol. 69, no. 11, pp. 11560–11568, Nov. 2022.

[3] A. Afshari, M. Karrari, H. Baghaee, and G. Gharehpetian, "Distributed fault-tolerant voltage/frequency synchronization in autonomous AC microgrids," *IEEE Trans. Power Syst.*, vol. 35, no. 5, pp. 3774–3789, Sept. 2020.

[4] X. Ge, Q.-L. Han, J. Wang, and X.-M. Zhang, "A scalable adaptive approach to multi-vehicle formation control with obstacle avoidance," *IEEE/CAA J. Autom. Sinica*, vol. 9, no. 6, pp. 990–1004, Jun. 2022.

[5] D. Ding, Z. Wang, and Q.-L. Han, "A scalable algorithm for event-triggered state estimation with unknown parameters and switching topologies over sensor networks," *IEEE Trans. Cyber.*, vol. 50, no. 9, pp. 4087–4097, Sept. 2020.

[6] M. Tucci, S. Riverso, J. Vasquez, J. Guerrero, and G. Ferrari-Trecate, "A decentralized scalable approach to voltage control of DC islanded microgrids," *IEEE Trans. Control Syst. Technol.*, vol. 24, no. 6, pp. 1965–1979, Nov. 2016.

[7] M. Tucci and G. Ferrari-Trecate, "A scalable, line-independent control design algorithm for voltage and frequency stabilization in AC islanded microgrids," *Automatica*, vol. 11, p. 108577, 2020.

[8] M. Zhai, Q. Sun, R. Wang, B. Wang, S. Liu, and H. Zhang, "Fully distributed fault-tolerant event-triggered control of microgrids under directed graphs," *IEEE Trans. Netw. Sci. Eng.*, vol. 9, no. 5, pp. 3570–3579, 2022.

[9] M. Shahab, B. Mozafari, S. Soleymani, N. Dehkordi, H. Shourkaei, and J. Guerrero, "Distributed consensus-based fault tolerant control of islanded microgrids," *IEEE Trans. Smart Grid*, vol. 11, no. 1, pp. 37–47, Jan. 2020.

[10] M. Ye, D. Li, Q.-L. Han, and L. Ding, "Distributed Nash equilibrium seeking for general networked games with bounded disturbances," *IEEE/CAA J. Autom. Sinica*, vol. 10, no. 2, pp. 376–387, 2023.

[11] M. Ye, Q.-L. Han, L. Ding, and S. Xu, "Distributed Nash equilibrium seeking in games with partial decision information: A survey," *Proc. IEEE*, vol. 111, no. 2, pp. 140–157, 2023.